Dynamic and nonlinear properties of epitaxial quantum-dot lasers on silicon operating under long- and short-cavity feedback conditions for photonic integrated circuits

Bozhang Dong*
LTCI, Télécom Paris, Institut Polytechnique de Paris, 19 Place Marguerite Perey, 91120 Palaiseau, France

Jun-Da Chen and Fan-Yi Lin
Institute of Photonics Technologies, Department of Electrical Engineering, National Tsing Hua University, Hsinchu 300, Taiwan

Justin C. Norman and John E. Bowers
Department of Electrical and Computer Engineering, University of California, Santa Barbara, California 93106, USA

Frédéric Grillot†
LTCI, Télécom Paris, Institut Polytechnique de Paris, 19 Place Marguerite Perey, 91120 Palaiseau, France
and Center for High Technology Materials, University of New Mexico, Albuquerque, New Mexico, 87106, USA

(Received 23 September 2020; accepted 1 March 2021; published 12 March 2021)

This work reports on an investigation of the dynamics of 1.3 μm epitaxial quantum dot (QD) lasers on silicon subject to delayed optical feedback. Operating the device under different feedback conditions, we experimentally identify various dynamical states of periodic oscillations. In the long-cavity feedback regime, the device remains chaos-free up to ≈70% (−1.55 dB) feedback strength. This remarkable result is in agreement with prior studies and is attributed to the particular design and properties of the QD-based active region. Shortening the external cavity length to the short-cavity regime being on the scale of photonics integrated circuits (PICs), the onset of periodic oscillations only takes place under extremely high feedback strength, which is much higher than those in PICs. The devices studied exhibit strong resistance to chip-scale back reflections in absence of any unstable oscillation. Our results also demonstrate that p doping is an efficient technique to further improve the feedback tolerance. These results point out the potential of QD lasers as an on-chip light source not requiring an optical isolator and gives insights for developing ultrastable silicon transmitters for PIC applications.

DOI: 10.1103/PhysRevA.103.033509

I. INTRODUCTION

Monolithic photonic integration is important for compact, robust, and energy-efficient transceivers, which are important for the high-speed telecommunication industry, next generation datacom transceivers [1,2], and advanced LIDAR systems [3] applied to self-driving automobiles [4]. In particular, silicon photonics benefits from the mature complementary-metal-oxide-semiconductor (CMOS) industry and paves the way for low-cost, small-footprint and large-scale photonic integrated circuits (PICs) [5]. Due to the charge-carrier confinement in three spatial dimensions, quantum dots (QDs) used as a gain media can offer superior continuous-wave properties over their quantum well (QW) and bulk counterparts [6,7], which make them highly interesting for PIC applications. Recent studies have demonstrated that QD lasers directly grown on silicon substrates exhibit high performance with low threshold current [8], high gain properties [9], remarkable temperature stability [10], low relative intensity noise (RIN) [11,12] and large reflection insensitivity [13,14]. All those features are of paramount importance for the integration of stable and isolator-free silicon-based transmitters in PICs with error-free transmission [7,13].

The nonlinear dynamics of semiconductor lasers subject to external optical feedback has been intensively studied. Prior studies indicated that the external optical feedback operation could lead to several dynamical regimes [15–17] whose presence depends on the external cavity length and feedback strength. In particular, it is known that chaotic oscillations, named coherence collapse, can highly destabilize the laser performance [18,19]. In practical optical fiber communication systems, the maximum reflection strength from optical connectors is estimated to be as large as 13% [20]; a criteria from IEEE 802.3ah suggests that the reflection tolerance of an optical interconnect should be higher than −26 dB [21]. In this context, developing reflection-resistant optical transmitters becomes significant to overcome the issues from chip-scale back reflections, since on-chip optical isolators of poor-performance and high-cost are no longer obligatory. Our previous work has already discussed the optical feedback dynamics of silicon QD lasers in the long-cavity regime (LCR) [14,19], in which a high degree of stability of such lasers was revealed without any chaotic oscillations. In addition, compared with QD lasers operating on the excited state (ES),

*bozhang.dong@telecom-paris.fr
†frederic.grillot@telecom-paris.fr

those operating on sole ground state (GS) are also better candidates for isolator-free PIC applications, owing to their stronger damping of the relaxation oscillations [19,22]. However, to understand what really happens on the scale of a PIC, an in-depth investigation of the optical feedback dynamics from long- to short-cavity regimes (SCR) is necessary to reach a comprehensive analysis of the reflection sensitivity of silicon QD lasers. In a practical case, the intrachip and interchip scale is on the order of micrometers and centimeters, respectively [23].

This work reports on the dynamics of a 1.3 μm epitaxial InAs/GaAs QD Fabry-Perot (FP) laser on silicon operating under various feedback conditions. In particular, by analyzing the full transition from SCR to LCR, our results confirm that the QD device still exhibits a very strong resistance to external optical feedback without showing any chaotic oscillations, even at the maximum feedback strength of $\approx$70% (-1.55 dB). Such remarkable features are attributed to the material properties of the QDs, leading to a small linewidth enhancement factor [24,25], a strong damping [7] and sole GS lasing [22]. Nevertheless, by tightly controlling the feedback parameters from SCR to LCR, various dynamical states such as regular pulse package (RPP), period-one (P1), quasiperiod-one (Q1) and quasiperiodic (QP) oscillations are identified. Our previous work in the LCR demonstrated that the feedback insensitivity of QD laser was improved by applying p-type doping in the active region [10]. In this work, we investigate how p doping affects the feedback sensitivity of silicon QD lasers in full transition from SCR to LCR. To do so, another device grown with the same QDs but without p-modulation doping in the active region is used for comparison. However, note that the facet reflectivities of the p-doped laser are left as-cleaved, which are much lower than those of the undoped device. From both devices, the tolerance for optical feedback is much enhanced by shortening the external cavity length from LCR to SCR. In other words, they exhibit strong resistance to interchip scale back reflection in absence of any unstable oscillations. Moreover, these results turn out that the reflection resistance of device can be further improved on the intrachip scale. In agreement with the results reported in Ref. [10], the p-doped device generally shows a higher degree of stability despite being much more open to the external world with as-cleaved facets. As opposed to that, the undoped laser has much larger power reflectivities on both facets, which means that, in this case, the light from the external cavity is not strongly coupled with the QD active medium. Therefore, the better performance of the p-doped device is purely attributed to the p doping. The present study brings now a detailed understanding of the nonlinear dynamics of multimode QD lasers on silicon, which gives insights for developing ultrastable silicon transmitters for isolator-free PIC applications.

II. EXPERIMENTAL CONFIGURATION

In the QD active region, the valence states are relatively less confined than the highly separately conduction-band states due to the heavier effective mass of holes. In this case, the rapid hole thermalization becomes one of the main mechanisms causing the gain to be temperature sensitive.

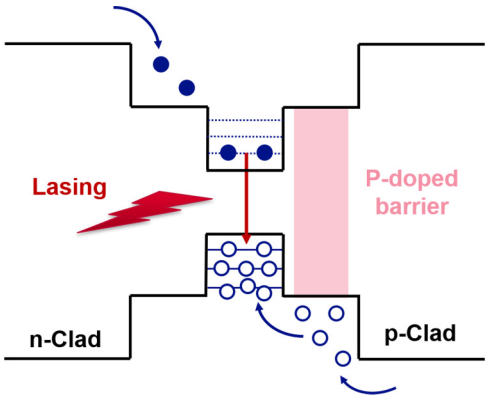

FIG. 1. Schematic illustration of the radiation process in a dot-in-a-well heterostructure with p-doped barrier.

Consequently, when QDs are undoped, the total charge density in the active layer increases in order to obtain a sufficient hole population in the QD ground state. However, in order to achieve a population inversion, the charge neutrality must also increase the total number of electrons, hence leading to a higher radiative current along with a reduced differential gain. Although p doping was already used in QW devices to mitigate the problem of closely spaced hole subbands, it can also be applied to QD lasers to overcome the broadening of the hole population and optimize the performance of QDs in terms of thermal stability. Figure 1 schematically illustrates the optically induced carrier transitions and energy levels in a layer of p-doped dot-in-a-well heterostructure. As injected electrons have a high probability of residing only in the QD GS, the large concentration of holes ensures that the injected electrons always find GS holes with which to recombine. Let us stress that the n-doped active region does not offer similar advantages either to increase the differential gain or the thermal stability. Indeed, once the electron state is full, the increase in gain is limited because it comes from the sole injection of holes into the GS holes which is a very slow process whereby holes are thermally distributed over a number of levels. Recent studies reveal that the p-doping technique is beneficial for reducing the carrier density required to achieve a certain quasi Fermi-level separation, hence resulting in the improvement of modal gain and differential gain. It also decreases the linewidth enhancement factor which is of first importance to improve high-temperature lasing characteristics, reliability of QD lasers on silicon as well as intensity noise properties [10,26]. Moreover, the p-doped QD lasers are touted for their better resistance against optical feedback with a critical feedback level beyond that of the undoped case [10]. This last feature is mostly attributed to the reduction of the linewidth enhancement factor in presence of p-doping. It may also be explained by the slight increase of the Shockley-Read-Hall (SRH) recombination rate especially at a high p-doping concentration ($\geqslant 10^{18}$ cm^{-3}), the latter is directly linked to the laser's damping factor hence the feedback sensitivity [27]. Hereinafter, we confirm the importance of p doping on the optical feedback performance of QD lasers on silicon.

In this study, both the QD devices presented in the following experiments are designed for emission on GS at 1310 nm

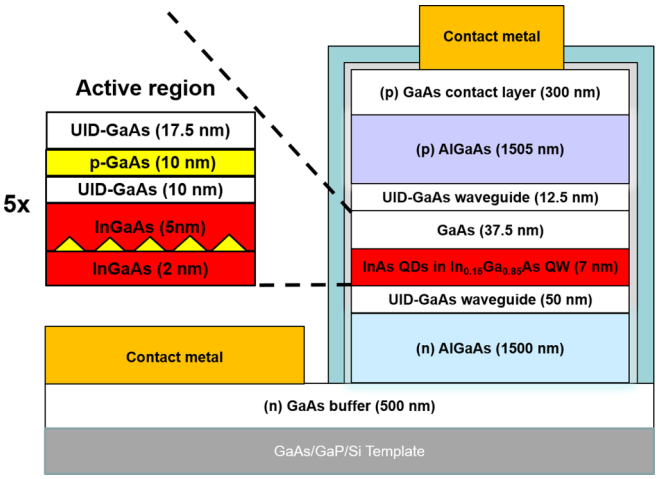

FIG. 2. Schematic illustration of the laser epitaxial structure; the close-up on the left depicts one period of the active region of the p-doped QD laser.

at room temperature, and their epitaxial structure based on the typical design is depicted in Fig. 2. The active region consists of five periods of InAs QDs embedded in $In_{0.15}Ga_{0.85}As$ QWs. The QD density is 6.5×10^{10} cm^{-2} with photoluminescence (PL) full width at half maximum below 30 meV. In the p-doped device, each dot layer is separated by a 37.5 nm GaAs spacer, in which a 10-nm-thick 5×10^{17} cm^{-3} p-type material layer is added to optimize the laser performance including the improvement of modal gain and thermal stability [26]; whereas for the undoped one, the p doping is absent. The whole structure of active region is then directly grown on an on-axis (001) GaP/silicon wafer in a Veeco Gen-II molecular-beam epitaxy chamber. Further details of the epitaxial growth are available elsewhere [9].

The p-doped QD laser is fabricated with standard dry etch and electron-beam metal deposition techniques. Its FP cavity is 1.35 mm long, with 3.5-μm-wide ridges deeply etched through the active region and two top metal contacts used for electrical injection. To improve the feedback strength in the following experiments, both facets of this laser are left as-cleaved with reflectivities of 32%. In comparison with the p-doped laser, another device grown from the same techniques except for the active region being undoped is investigated. To optimize the lasing efficiency, its front and rear facets of are applied by SiO_2/Ta_2O_5 coatings to give reflectivities of 60% and 99%, respectively. Other structure details can be found in Refs. [7,10]. In this study, the p-doped laser exhibits strong resistance to optical feedback without showing any unstable oscillation at room temperature (20 °C), in this case the experiments based on this device described hereinafter are performed at 30 °C where the destabilization takes place. On the other hand, experiments on the undoped laser are effected at 20°C. In this study, we do not investigate the optical feedback operation on those devices at a higher temperature, given that the undoped QD laser exhibits a poor thermal stability due to the aforementioned rapid hole thermalization, whose presence limits its operation at a higher temperature. In particular, the output power is too limited for conducting experiments over 30 °C. A previous study also demonstrated that an undoped QD laser suffers from both intensity and wavelength fluctuations under optical feedback at 30 °C [10]. Figure 3(a) depicts the multimode optical spectrum of the p-doped QD laser at 160 mA; such a condition is marked by the red bullet on the light-current curve measured at 30 °C shown in the inset. As shown, the p-doped laser with threshold current I_{th} of 36 mA exhibits sufficient output power over 15 mW. To avoid power roll-over, the bias current in the following experiments is fixed at 125 mA ($3.4I_{th}$) and 160 mA ($4.4I_{th}$) to maximize the output power. It is worth noting here that the emission on ES does not take place up to $5I_{th}$; such a large ES-to-GS lasing threshold ratio is also beneficial for strengthening the resistance against external optical feedback for QD lasers [19]. For comparison, a similar bias-to-threshold ratios as the p-doped device are kept for the whole investigation of the undoped laser dynamics.

Figure 3(b) depicts the free-space optical feedback setup for the p-doped QD laser. The device is mounted on a suspended optical table to minimize the environmental perturbations. Owing to the symmetric as-cleaved coating design of this laser, the setup is thus separated into two parts: One part at the side of front facet is for optical feedback operation and the other at the side of rear facet is for light detection and analysis. The free-space external cavity was located outside of the front facet of laser, in which the lasing emission is first collimated and then reflected by a movable mirror mounted on an optical rail. The latter allows us to adjust the external cavity length L_{ext} from 4 cm (minimum, blue) up to 50 cm (maximum, red). In a technical view, reducing the L_{ext} to a few centimeters is complicated in free-space operation, hence well arranging the experimental apparatuses is necessary. In this study, the SCR and LCR is defined as the ratio of f_{RO}/f_{ext} being <1 or >1, respectively [28], with f_{RO} being the relaxation oscillation frequency of the solitary laser and $f_{ext} = c/2L_{ext}$ the frequency of the external cavity. Thus, for the p-doped laser, f_{RO} being 2 and 1.5 GHz at 160 and 125 mA, respectively, ensure the corresponding ratio of f_{RO}/f_{ext} ranging from 0.5 to 7 and from 0.4 to 5, which finely probes the laser dynamics in transition from SCR to LCR. For each measurements at different L_{ext}, the focus of the collimator needs to be readjusted in order to precisely send the coupled light onto the mirror. In this configuration, the feedback strength r_{ext} being defined as the ratio of the returning power to the laser output power is controlled by a free-space variable optical attenuator (VOA), which gives extra loss in the external cavity thus allows us to slightly modify the r_{ext}. In this setup, the r_{ext} taking into account the coupling loss between the facet and the external cavity ranges from 0.04% (−34 dB) to ≈70% (−1.55 dB), with an accuracy better than 0.01%. On the light detection path, laser emission from the rear facet is first coupled by an AR coated lens-end fiber and isolated to avoid any back reflection from the setup. The coupled light is then sent to an electrical spectrum analyzer (ESA) and an oscilloscope (OSC) for further analysis. The experimental setup for the undoped device only emitting from front facet is a little different from that for the p-doped one. In this case, a 50/50 free-space beam splitter (BS) is placed outside of the collimator in order to divert 50% output light into the detection path (setup not shown in this paper). As such, the maximum r_{ext} in the external cavity taking into account the loss from the BS is limited to ≈22%. Adjusting

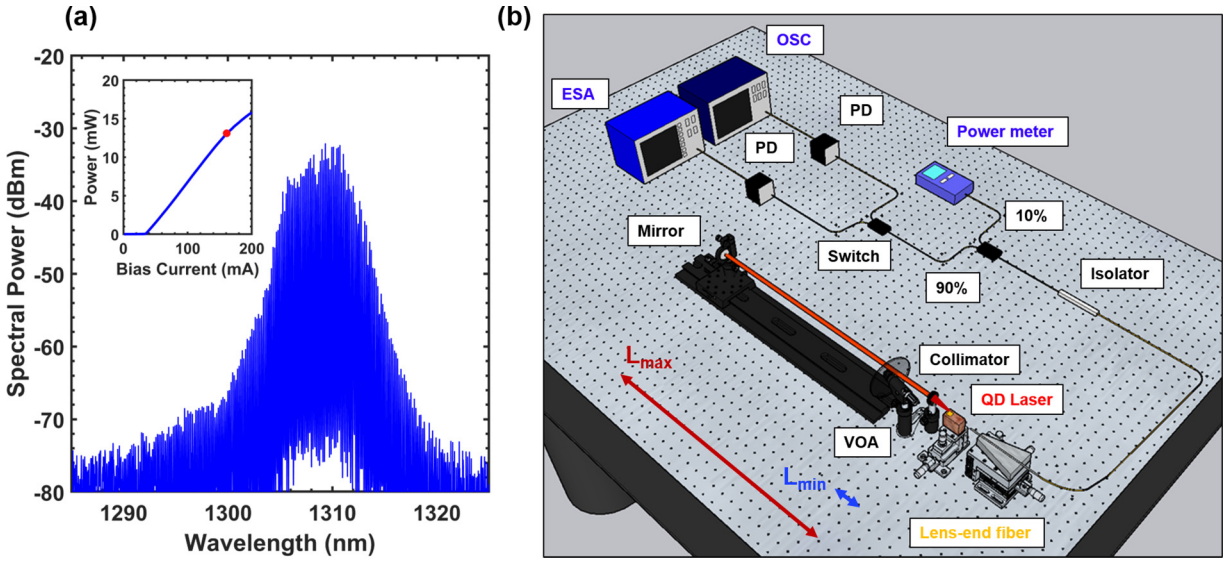

FIG. 3. (a) Optical spectrum on of the p-doped laser at 160 mA ($4.4I_{th}$, red marker). The inset depicts the light-current characteristics measured at 30 °C. (b) Schematic of the experimental setup for measurement of the QD lasers. VOA, variable optical attenuator; PD, 12 GHz photodiode; ESA, electrical spectrum analyzer; OSC, oscilloscope.

the L_{ext} ranging from 4 cm to 50 cm, corresponding f_{RO}/f_{ext} of the undoped laser therefore ranges from 0.8 to 10, where its f_{RO} is 3 GHz at $3I_{th}$. Further details of this experimental setup can be found in Ref. [29].

III. RESULTS AND DISCUSSIONS

The results displayed in this section are mainly taken from the p-doped QD laser. Extending L_{ext} from SCR to LCR, different self-pulsation dynamics of the device are identified. Figure 4(a) depicts the radio-frequency (rf) spectrum (left column), time series (middle column), and phase portraits (right column) of the device operating at 160 mA with $r_{ext} = 68.2\%$ (−1.66 dB) and L_{ext} being 4 cm ($f_{ext} = 3.75$ GHz). Corresponding ratio of f_{RO}/f_{ext} being 0.5 indicates that the f_{ext} was largely beyond the f_{RO} of the QD laser, where the RPP takes place. As shown in Figs. 4(a-ii), a series of regular pulses oscillating at f_{ext} are modulated by a slower envelope, whose repetition frequency f_{RPP} being 55 MHz is clearly depicted in the inset of Fig. 4(a-i). On the other hand, the inset of Fig. 4(a-ii) highlights the fast oscillations at f_{ext} within one envelop. It is worth noting here that such a large ratio of f_{ext}/f_{RPP} being 68 is much more than those observed on other devices including QW and QD lasers [28,30,31]. Moreover, the phase portraits shown in Fig. 4(a-iii) reveals that the slow oscillation frequency coincident with f_{RPP} does not bring huge discrepancy from the single-frequency pulsations since only one cycle can be identified, however, the laser system suffers from strong instabilities induced by the feedback phase. Note that the slow oscillations at the border of RPP regime exhibits sustained instability on temporal scale, whose presence performs a variable f_{RPP} as the time changes. To overcome this issue, it would be important to further reduce the external cavity to fully probe the pure RPP regime from which the laser output can resemble to that of a mode-locked laser. Extending the L_{ext} to 6.5 cm while ensuring the same $r_{ext} = 68.2\%$, the device enters into the P1 state; the corresponding rf spectrum, time series and phase portraits are shown in Fig. 4(b). In this case, the ratio of f_{RO}/f_{ext} being ≈0.9 indicates that the QD laser still operates in the SCR. At this stage, the regular pulses oscillating at $f_{ext} = 2.3$ GHz are shown in Fig. 4(b-ii), the higher harmonics of f_{ext} are identified in Fig. 4(b-i). Compared with the phase portraits of RPP, those of P1 shown in Fig. 4(b-iii) reflect the uniformity of the single-frequency oscillations by exhibiting a pretty regular cycle. Further increasing the ratio of f_{RO}/f_{ext} to ≈2 by extending the L_{ext} to 15 cm, the device therefore operates in LCR. Still ensuring the maximum $r_{ext} = 68.2\%$, both the f_{ext} and the self-pulsation frequency f_{sp} shown in Fig. 4(c-i) contribute to shape the waveform [Fig. 4(c-ii)], thus leading the device into the QP state. When L_{ext} is shorter than the coherence length L_{coh} of laser, f_{sp} is coincident with the higher harmonics of f_{ext}, thus exhibiting a strong dependence of L_{ext}. Corresponding discussions will be performed in this paper later on. On the other hand, the f_{sp} is observed to fluctuate around f_{RO} as L_{ext} changes. The difference between QP and P1 can be clearly seen from the phase portraits [Fig. 4(c-iii)] through the exhibited two cycles, which is the sign of two-frequency oscillations. In LCR, it is worth stressing that the f_{sp} should coincide with the f_{RO} in free running operation. Nevertheless, our following results demonstrate that f_{sp} varies with the change in L_{ext}, whose presence depends on the mode competition between the linear modes near f_{RO} [32]. The influence of L_{ext} on f_{sp} can be eliminated once L_{ext} exceeds the coherence length. In the case of QD lasers with typically narrow rf linewidth below 200 kHz [33,34], their coherence length is about several hundred meters [22,35]. In this study, the r_{ext} effect on laser dynamics is also investigated. To do so, r_{ext} is decreased to 33% (−4.8 dB) while fixing $L_{ext} = 15$ cm, the device becomes more stable and enters into the Q1 state. Different from the P1 state described in prior studies [36,37] and aforementioned in this section, the oscillation frequency coincident with f_{ext} [Fig. 4(d-i)] does not show any higher harmonic. Note that the rf intensity of the f_{ext} is quite low,

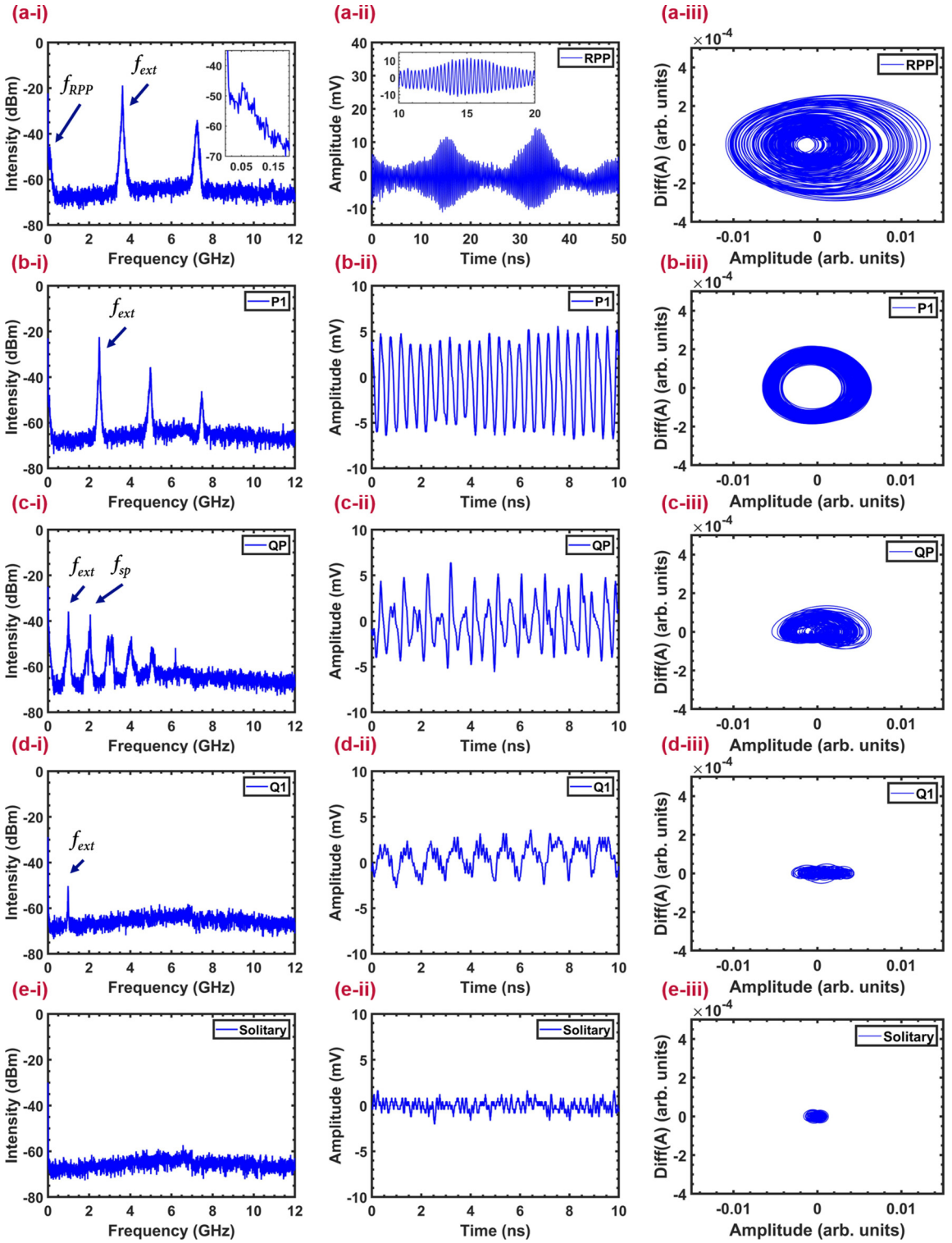

FIG. 4. Electrical spectra (left), time series (middle), and phase portraits (right) of the p-doped QD laser with (r_{ext}, L_{ext}) = (a) (68.2%, 4 cm), (b) (68.2%, 6.5 cm), (c) (68.2%, 15 cm), (d) (33%, 15 cm), and (e) solitary, when it was biased to 160 mA. f_{ext}, frequency of the external cavity; f_{sp}, self-pulsation frequency.

thus the waveform shown in Fig. 4(d-ii) is largely influenced by the high-frequency noise, whose presence makes the corresponding phase portraits [Fig. 4(d-iii)] hard to distinguish from those at the solitary state (without feedback). As a reference, the spectra of the solitary state are shown in Fig. 4(e).

In this study, it is worth noting that the QD laser does not exhibit any chaotic oscillations from SCR to LCR, even if it operates under strong optical feedback with $r_{ext} \simeq 70\%$. Prior studies revealed that the QW lasers suffered from strong instabilities against optical feedback, performed by generally exhibiting chaotic oscillations with r_{ext} below 5% in

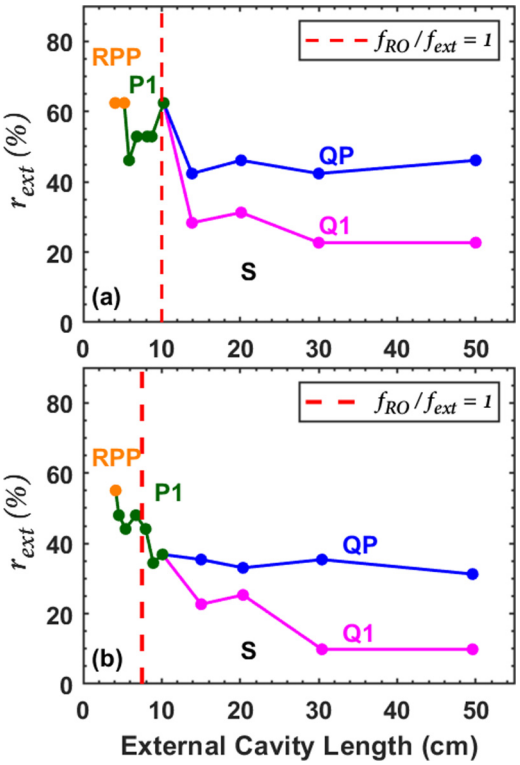

FIG. 5. Mappings of the dynamical states of the p-doped QD laser under different feedback conditions at (a) 125 mA and at (b) 160 mA. The vertical red dashed lines depict the boundaries of the SCR and the LCR.

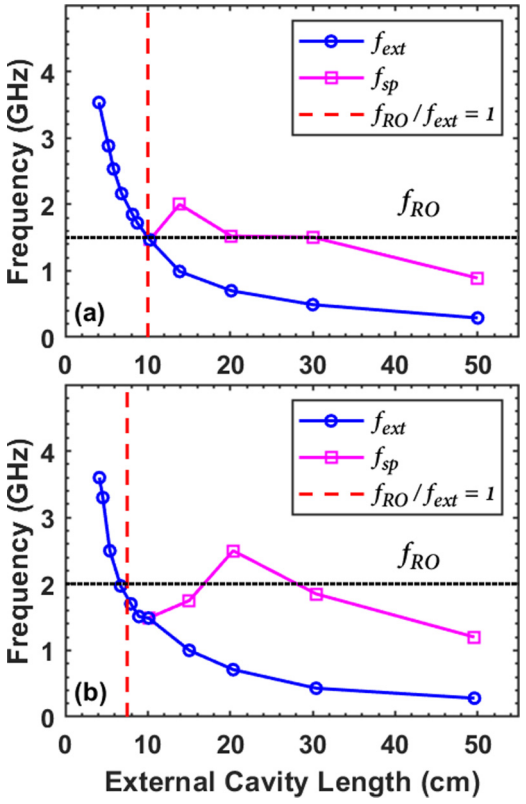

FIG. 6. The oscillation frequency f_{FO} (blue circle) and f_{SO} (magenta square) as a function of L_{ext} of the p-doped QD laser at (a) 125 mA and at (b) 160 mA, the horizontal dotted black lines illustrate the free-running f_{RO}. The vertical dashed red lines depict the boundaries of the SCR and LCR.

both SCR and LCR [13,32]. Those features definitely limited their applications for isolator-free integration. In this context, the chaos-free QD laser reported in this paper is important to be applied in PICs to improve their robustness against chip-scale back reflections. It is worth stressing that the remarkable feedback resistance of the device studied are attributed to some peculiar properties of QDs. Compared with QW lasers, our previous work performed in the LCR has demonstrated that the enhanced feedback insensitivity of silicon-based QD devices originated from the large damping rate over 30 GHz [7] and the near-zero linewidth enhancement factor [24,38]; in addition, the p-type doping in the active region is also beneficial for further improving the tolerance to external optical feedback, corresponding discussions are available in the end of this paper. On the other hand, the aforementioned periodic oscillations in the p-doped laser subject to optical feedback exhibit strong dependence on the L_{ext}, which are also studied in this work.

By increasing the r_{ext} from 0.04% to ≈70%, one can extract the boundaries associated with the different periodic states both in SCR and LCR. To do so, the onset of each periodic oscillation is defined as the corresponding excited oscillation frequency being 5 dB above the free-running noise level. Figures 5(a) and 5(b) depict the aforementioned boundaries as a function of the L_{ext}, when the device operates at 125 mA ($3.4I_{th}$) and 160 mA ($4.4I_{th}$), respectively. The vertical dashed red lines corresponding to the condition $f_{RO}/f_{ext} = 1$ are performed to separate the SCR and LCR. To improve the precision, measurements are performed by varying L_{ext} every centimeter in the SCR while larger steps are taken in the LCR. Our results demonstrate that the device becomes more stable against optical feedback at a lower bias current where the region of the steady state (S, marked in black) expands and r_{ext} required for the laser to excite instability increases. This feature is attributed to the reduced linewidth enhancement factor above threshold [10]. In both cases, the boundaries associated with unstable oscillations exhibit strong undulations in SCR, whose presences are attributed to the coupling degree between the internal and external cavity modes [39]. On the other hand, the QD laser is less stabilized with a small fraction of optical feedback in LCR, thus the instability boundaries progressively become rather independent of L_{ext}. Operating in the SCR, our results demonstrate that the RPP oscillations (marked in orange) only take place in the ultra-short delay region where $f_{RO}/f_{ext} < 0.5$, since the influence of the feedback phase is much enhanced in this regime [28]. Extending L_{ext} to $f_{RO}/f_{ext} \simeq 1$, the device only exhibits P1 oscillations (marked in green). It is worth stressing that the QD laser remains in the S region with r_{ext} below 35% in SCR. More dynamical states are identified in LCR. Increasing the r_{ext}, the device remains in the S region under weak r_{ext}, until it oscillates at f_{ext} thus enters into Q1 state (marked in magenta), then the f_{RO} is excited, performing the onset of QP oscillations (marked in blue).

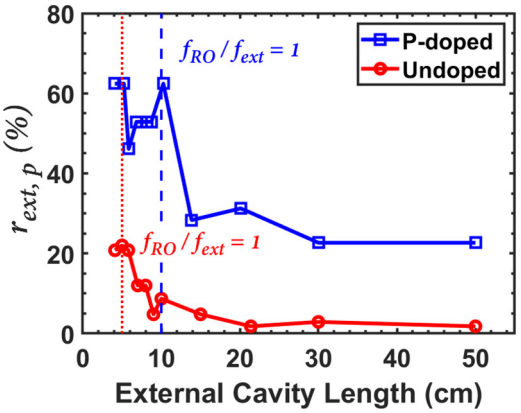

FIG. 7. The onset of periodic oscillations $r_{\text{ext},p}$ associated with L_{ext} of the p-doped (blue squares) and undoped (red circles) QD laser. Both devices were biased at $\approx 3\text{I}_{\text{th}}$. The vertical dashed blue and dotted red lines depict the boundaries of the SCR and LCR of the p-doped and undoped device, respectively.

To understand the periodic stability enhancements taking place in the condition satisfying $L_{\text{ext}} = mc/2f_{RO}$ ($f_{RO}/f_{\text{ext}} = m$, m is an integer), Figs. 6(a) and 6(b) display the excited f_{sp} as a function of L_{ext} at 125 mA ($3.4 \times I_{\text{th}}$) and 160 mA ($4.4 \times I_{\text{th}}$), respectively. The vertical dashed red lines corresponding to $f_{RO}/f_{\text{ext}} = 1$ is once again indicating the separation of regimes. In agreement with prior studies, f_{sp} coincides with f_{ext} (marked in blue circle) in SCR [40], whereas it oscillates at both f_{ext} (marked in magenta squares) and $\approx f_{RO}$ (marked in blue circles) in the LCR. It is worth stressing that the strong mode competition taking place in f_{RO}/f_{ext} being an integer is indeed beneficial for enhancing the feedback insensitivity by improving the $r_{\text{ext},p}$ shown in Figs. 5(a) and 5(b) [39]. Nevertheless, the extension of the L_{ext} within one period is found to not only largely degrade the laser stability against optical feedback (lower $r_{\text{ext},p}$) but also decrease f_{FO}. These features are attributed to the decrease of the damping factor with increasing L_{ext} [41]. In addition, the undulations of both f_{sp} and r_{ext} associated with the onset of unstable oscillations in LCR reveal that the QD laser still operates in the coherent feedback regime, in which the laser dynamics is largely influenced by the feedback phase. This coherence would be eliminated once further increasing the ratio f_{RO}/f_{ext} until f_{FO} coincident with free-running f_{RO} becomes independent of L_{ext}.

Prior studies on p-type doping in QD lasers revealed that it is beneficial for enhancing the laser performance, including higher material gain [9], larger modulation bandwidth [42], and better thermal stability [10]. Our previous work also demonstrated that the feedback insensitivity of QD laser in LCR could be improved by applying this technique [10]. In this work, we go an important step beyond by investigating the p-doping effect on the feedback sensitivity in SCR, where the feedback conditions closely resemble those of PICs. Figure 7 depicts the onset to periodic oscillations $r_{\text{ext},p}$ as a function of L_{ext} for the p-doped (blue squares) and undoped (red circles) QD laser at $\approx 3I_{\text{th}}$; the corresponding boundaries of the SCR and LCR are marked by dashed or dotted lines in the same colors. As aforementioned, the operation temperature of the p-doped and undoped device is 30 °C and 20 °C, respectively. It is worth stressing that both the as-cleaved facets of the p-doped device make it more open to the external world than the undoped one, which is not always favorable for maintaining the tolerance to optical feedback [14]. Nevertheless, the p-doped laser clearly displays a much stronger resistance to optical feedback than its counterpart even at a higher operation temperature, hence exhibiting a higher $r_{\text{ext},p}$ in full transition from the SCR to the LCR [10]. This remarkable performance improvement is mainly attributed to the reduced linewidth enhancement factor owing to the p-doping [10]. Importantly, both QD lasers studied exhibit remarkable tolerance for interchip-scale back reflection. The improvement of feedback resistance with decreasing L_{ext} shows that these devices can still be reflection resistant on the intrachip scale. Furthermore, although the p-doped QD laser has a higher threshold current [9] and a lower damping rate [10], its stronger stability against back reflection fits very well the needs for high performance PICs operating without an optical isolator.

IV. CONCLUSIONS

This work brings fundamental insight on the multimode optical feedback dynamics of InAs/GaAs QD lasers epitaxially grown on silicon. In agreement with prior studies, our results demonstrate that the silicon QD laser displays a strong resistance to optical perturbations without showing any chaotic pulsations whatever the external cavity length and feedback strength was. Such a remarkable feature is attributed to the very large damping factor, the near-zero linewidth enhancement factor, and the participation of p-doping in the active region, which prevent it from any chaotic oscillations even within extreme feedback conditions. In this study, the evolution of the extracted boundaries associated with different dynamical states and the excited periodic frequencies unveil a clear dependence on L_{ext} in SCR, while the system becomes rather independent of the feedback phase in the LCR. Compared with the reflection-sensitive QW lasers, it is worth stressing that the observed strong tolerance for optical feedback in the SCR is much beyond the IEEE 802.3ah standard, hence this study highlights the potential of epitaxial QD lasers on silicon as ultrastable light sources applicable on the scale of PICs. As a conclusion, these results provide useful guidelines for developing QD laser based PICs without the need of optical isolators, which is an important solution for realizing low-cost, energy-efficient data centers and supercomputer applications. The analysis of the pulsing states is also strongly driven by the growing interest in microwave photonic technology from which exciting perspectives can be envisioned such as the fabrication of an integrated device in a PIC capable of delivering microwave signals without the need of electrical modulation.

ACKNOWLEDGMENTS

Authors acknowledge the financial support of Advanced Research Projects Agency - Energy contract DE-AR0001039, the Institut Mines-Télécom, and Y.S. Liu Global Talent Scholarship, and Ministry of Science and Technology, Taiwan (MOST) (109-2218-E-007-031).

[1] A. Vahdat, H. Liu, X. Zhao, and C. Johnson, The emerging optical data center, in *Optical Fiber Communication Conference/National Fiber Optic Engineers Conference 2011, Los Angeles, California United States* (Optical Society of America, 2011), p. OTuH2.

[2] D. Nikolova, S. Rumley, D. Calhoun, Q. Li, R. Hendry, P. Samadi, and K. Bergman, Scaling silicon photonic switch fabrics for data center interconnection networks, Opt. Express **23**, 1159 (2015).

[3] A. Martin, D. Dodane, L. Leviandier, D. Dolfi, A. Naughton, P. O'Brien, T. Spuessens, R. Baets, G. Lepage, P. Verheyen *et al.*, Photonic integrated circuit-based FMCW coherent LiDAR, J. Lightwave Technol. **36**, 4640 (2018).

[4] W. Xie, T. Komljenovic, J. Huang, M. Tran, M. Davenport, A. Torres, P. Pintus, and J. Bowers, Heterogeneous silicon photonics sensing for autonomous cars, Opt. Express **27**, 3642 (2019).

[5] R. Jones, P. Doussiere, J. B. Driscoll, W. Lin, H. Yu, Y. Akulova, T. Komljenovic, and J. E. Bowers, Heterogeneously integrated InP/silicon photonics: Fabricating fully functional transceivers, IEEE Nanotechnol. Mag. **13**, 17 (2019).

[6] A. Ukhanov, A. Stintz, P. Eliseev, and K. Malloy, Comparison of the carrier induced refractive index, gain, and linewidth enhancement factor in quantum dot and quantum well lasers, Appl. Phys. Lett. **84**, 1058 (2004).

[7] J. Duan, H. Huang, B. Dong, J. C. Norman, Z. Zhang, J. E. Bowers, and F. Grillot, Dynamic and nonlinear properties of epitaxial quantum dot lasers on silicon for isolator-free integration, Photonics Res. **7**, 1222 (2019).

[8] D. Jung, Z. Zhang, J. Norman, R. Herrick, M. Kennedy, P. Patel, K. Turnlund, C. Jan, Y. Wan, A. C. Gossard *et al.*, Highly reliable low-threshold inas quantum dot lasers on on-axis (001) Si with 87% injection efficiency, ACS Photonics **5**, 1094 (2017).

[9] J. C. Norman, D. Jung, Z. Zhang, Y. Wan, S. Liu, C. Shang, R. W. Herrick, W. W. Chow, A. C. Gossard, and J. E. Bowers, A review of high-performance quantum dot lasers on silicon, IEEE J. Quantum Electron. **55**, 1 (2019).

[10] H. Huang, J. Duan, B. Dong, J. Norman, D. Jung, J. E. Bowers, and F. Grillot, Epitaxial quantum dot lasers on silicon with high thermal stability and strong resistance to optical feedback, APL Photonics **5**, 016103 (2020).

[11] M. Liao, S. Chen, Z. Liu, Y. Wang, L. Ponnampalam, Z. Zhou, J. Wu, M. Tang, S. Shutts, Z. Liu *et al.*, Low-noise 1.3μmInAs/GaAs quantum dot laser monolithically grown on silicon, Photonics Res. **6**, 1062 (2018).

[12] J. Duan, Y. Zhou, B. Dong, H. Huang, J. C. Norman, D. Jung, Z. Zhang, C. Wang, J. E. Bowers, and F. Grillot, Effect of p-doping on the intensity noise of epitaxial quantum dot lasers on silicon, Opt. Lett. **45**, 4887 (2020).

[13] J. Duan, H. Huang, B. Dong, D. Jung, J. C. Norman, J. E. Bowers, and F. Grillot, 1.3-μm reflection insensitive InAs/GaAs quantum dot lasers directly grown on silicon, IEEE Photonics Technol. Lett. **31**, 345 (2019).

[14] F. Grillot, J. C. Norman, J. Duan, Z. Zhang, B. Dong, H. Huang, W. W. Chow, and J. E. Bowers, Physics and applications of quantum dot lasers for silicon photonics, Nanophotonics **9**, 1271 (2020).

[15] R. Tkach and A. Chraplyvy, Regimes of feedback effects in 1.5-μm distributed feedback lasers, J. Lightwave Technol. **4**, 1655 (1986).

[16] J. Mørk, J. Mark, and B. Tromborg, Route to Chaos and Competition between Relaxation Oscillations for a Semiconductor Laser with Optical Feedback, Phys. Rev. Lett. **65**, 1999 (1990).

[17] K. Petermann, External optical feedback phenomena in semiconductor lasers, IEEE J. Sel. Top. Quantum Electron. **1**, 480 (1995).

[18] D. Lenstra, B. Verbeek, and A. Den Boef, Coherence collapse in single-mode semiconductor lasers due to optical feedback, IEEE J. Quantum Electron. **21**, 674 (1985).

[19] H. Huang, J. Duan, D. Jung, A. Y. Liu, Z. Zhang, J. Norman, J. E. Bowers, and F. Grillot, Analysis of the optical feedback dynamics in InAs/GaAs quantum dot lasers directly grown on silicon, J. Opt. Soc. Am. B **35**, 2780 (2018).

[20] K. Park, J. Lee, J. H. Han, H. Cho, D. Jang, C. Park, K. Pyun, and J. Jeong, The effects of external optical feedback on the power penalty of DFB-LD modules for 2.5 GBs-1 optical transmission systems, Opt. Quantum Electron. **30**, 23 (1998).

[21] *IEEE Standard for Information technology–Local and metropolitan area networks–Part 3: CSMA/CD Access Method and Physical Layer Specifications Amendment: Media Access Control Parameters, Physical Layers, and Management Parameters for Subscriber Access Networks*, in IEEE Std 802.3ah-2004 (IEEE, 2002), pp.1–640.

[22] H. Huang, L.-C. Lin, C.-Y. Chen, D. Arsenijević, D. Bimberg, F.-Y. Lin, and F. Grillot, Multimode optical feedback dynamics in InAs/GaAs quantum dot lasers emitting exclusively on ground or excited states: Transition from short-to long-delay regimes, Opt. Express **26**, 1743 (2018).

[23] G. Roelkens, L. Liu, D. Liang, R. Jones, A. Fang, B. Koch, and J. Bowers, III-V/silicon photonics for on-chip and intra-chip optical interconnects, Laser Photonics Rev. **4**, 751 (2010).

[24] J. Duan, H. Huang, D. Jung, Z. Zhang, J. Norman, J. Bowers, and F. Grillot, Semiconductor quantum dot lasers epitaxially grown on silicon with low linewidth enhancement factor, Appl. Phys. Lett. **112**, 251111 (2018).

[25] W. W. Chow, Z. Zhang, J. C. Norman, S. Liu, and J. E. Bowers, On quantum-dot lasing at gain peak with linewidth enhancement factor $\alpha_h = 0$, APL Photonics **5**, 026101 (2020).

[26] J. C. Norman, Z. Zhang, D. Jung, C. Shang, M. Kennedy, M. Dumont, R. W. Herrick, A. C. Gossard, and J. E. Bowers, The importance of p-doping for quantum dot laser on silicon performance, IEEE J. Quantum Electron. **55**, 1 (2019).

[27] M. Saldutti, A. Tibaldi, F. Cappelluti, and M. Gioannini, Impact of carrier transport on the performance of QD lasers on silicon: A drift-diffusion approach, Photonics Res. **8**, 1388 (2020).

[28] T. Heil, I. Fischer, W. Elsäßer, and A. Gavrielides, Dynamics of Semiconductor Lasers Subject to Delayed Optical Feedback: The Short Cavity Regime, Phys. Rev. Lett. **87**, 243901 (2001).

[29] B. Dong, J.-D. Chen, H.-L. Tsay, H. Huang, J. Duan, J. C. Norman, J. E. Bowers, F.-Y. Lin, and F. Grillot, P-doping effect on external optical feedback dynamics in 1.3-micron InAs/GaAs quantum dot laser epitaxially grown on silicon, in *Semiconductor Lasers and Laser Dynamics IX* (International Society for Optics and Photonics, 2020), Vol. 11356, p. 113560C.

[30] A. Tabaka, K. Panajotov, I. Veretennicoff, and M. Sciamanna, Bifurcation study of regular pulse packages in laser diodes subject to optical feedback, Phys. Rev. E **70**, 036211 (2004).

[31] L.-C. Lin, C.-Y. Chen, H. Huang, D. Arsenijević, D. Bimberg, F. Grillot, and F.-Y. Lin, Comparison of optical feedback dynamics of InAs/GaAs quantum-dot lasers emitting solely on ground or excited states, Opt. Lett. **43**, 210 (2018).

[32] J. Ohtsubo, *Semiconductor Lasers: Stability, Instability and Chaos* (Springer-Verlag, Berlin Heidelberg, 2012), Vol. 111.

[33] J. Duan, H. Huang, Z. Lu, P. Poole, C. Wang, and F. Grillot, Narrow spectral linewidth in InAs/InP quantum dot distributed feedback lasers, Appl. Phys. Lett. **112**, 121102 (2018).

[34] T. Septon, A. Becker, S. Gosh, G. Shtendel, V. Sichkovskyi, F. Schnabel, A. Sengül, M. Bjelica, B. Witzigmann, J. P. Reithmaier, and G. Eisenstein, Large linewidth reduction in semiconductor lasers based on atom-like gain material, Optica **6**, 1071 (2019).

[35] L. A. Coldren, S. W. Corzine, and M. L. Mashanovitch, *Diode Lasers and Photonic Integrated Circuits* (John Wiley & Sons, Inc., Hoboken, New Jersey, 2012), Vol. 218.

[36] A. Murakami and J. Ohtsubo, Dynamics of semiconductor lasers with optical feedback from photorefractive phase conjugate mirror, Opt. Rev. **6**, 359 (1999).

[37] L.-C. Lin, S.-H. Liu, and F.-Y. Lin, Stability of period-one (P1) oscillations generated by semiconductor lasers subject to optical injection or optical feedback, Opt. Express **25**, 25523 (2017).

[38] Z. Zhang, D. Jung, J. C. Norman, W. W. Chow, and J. E. Bowers, Linewidth enhancement factor in InAs/GaAs quantum dot lasers and its implication in isolator-free and narrow linewidth applications, IEEE J. Sel. Top. Quantum Electron. **25**, 1 (2019).

[39] A. Murakami and J. Ohtsubo, Dynamics and linear stability analysis in semiconductor lasers with phase-conjugate feedback, IEEE J. Quantum Electron. **34**, 1979 (1998).

[40] J. P. Toomey, D. M. Kane, C. McMahon, A. Argyris, and D. Syvridis, Integrated semiconductor laser with optical feedback: Transition from short to long cavity regime, Opt. Express **23**, 18754 (2015).

[41] N. Gavra and M. Rosenbluh, Behavior of the relaxation oscillation frequency in vertical cavity surface-emitting laser with external feedback, J. Opt. Soc. Am. B **27**, 2482 (2010).

[42] D. G. Deppe, H. Huang, and O. B. Shchekin, Modulation characteristics of quantum-dot lasers: The influence of p-type doping and the electronic density of states on obtaining high speed, IEEE J. Quantum Electron. **38**, 1587 (2002).